



Received: 29 August 2014 – Accepted: 21 September 2014 – Published: 22 October 2014

Correspondence to: M. Van Rampelbergh (mvrampel@vub.ac.be)

Published by Copernicus Publications on behalf of the European Geosciences Union.

## CPD

10, 4149–4190, 2014

### A 500 year seasonally resolved $\delta^{18}\text{O}/\delta^{13}\text{C}$

M. Van Rampelbergh  
et al.

Title Page

Abstract

Introduction

Conclusions

References

Tables

Figures



Back

Close

Full Screen / Esc

Printer-friendly Version

Interactive Discussion



## Abstract

Speleothem  $\delta^{18}\text{O}$  and  $\delta^{13}\text{C}$  signals have already proven to enable climate reconstructions at high resolution. However, seasonally resolved speleothem records are still scarce and often difficult to interpret in terms of climate due to the multitude of factors that can affect the proxy signals. In this paper, a fast growing (up to  $2\text{ mm yr}^{-1}$ ) seasonally laminated speleothem from the Han-sur-Lesse cave (Belgium) is analyzed for its  $\delta^{18}\text{O}$  and  $\delta^{13}\text{C}$  values, layer thickness and changes in calcite fabric. The studied part of the speleothem covers the most recent 500 years as indicated by layer counting and confirmed by 20 U / Th-ages. Epikarst recharge occurs mainly in winter and lesser during spring and fall. a good correlation can be established between lower winter temperatures and lower winter precipitation (DJF) based on the measured data by the Belgian meteorological institute since 1833 indicating that a dry winter is also a cold winter. Colder and dryer winters cause lower winter recharge and generally drier conditions in the cave. Lower winter recharge decreases the amount of isotopically light ( $\delta^{18}\text{O}$ ) winter precipitation added to the epikarst in comparison to the heavier spring and fall waters, which leads to a net increase in  $\delta^{18}\text{O}$  value of the water in the epikarst. Increased  $\delta^{18}\text{O}$  values in the Proserpine are consequently interpreted to reflect colder and dryer winters. Higher  $\delta^{13}\text{C}$  signals are interpreted to reflect increased prior calcite precipitation (PCP) due to colder and dryer winters, when recharge is lower. Thinner layers and darker calcite relate to slower growth and occur when drip rates are low and when the drip water calcium ion concentration is low due to increased PCP, both caused by lower recharge during periods with colder and dryer winters. Exceptionally cold and dry winters cause the drip discharge to decrease under a certain threshold value inducing anomalies in the measured proxy records. Such anomalies occur from 1565 to 1610, from 1770 to 1800, from 1810 to 1860 and from 1880 to 1895 and correspond with exceptionally cold periods in proxy-based, historical and instrumental records and may relate to different factors such as negative winter NAO phases, lower solar irradiance and/or volcanic eruptions. When the discharge threshold is not reached, lower

## A 500 year seasonally resolved $\delta^{18}\text{O}/\delta^{13}\text{C}$

M. Van Rampelbergh  
et al.

[Title Page](#)

[Abstract](#)

[Introduction](#)

[Conclusions](#)

[References](#)

[Tables](#)

[Figures](#)



[Back](#)

[Close](#)

[Full Screen / Esc](#)

[Printer-friendly Version](#)

[Interactive Discussion](#)



**A 500 year seasonally resolved  $\delta^{18}\text{O}/\delta^{13}\text{C}$** M. Van Rampelbergh  
et al.[Title Page](#)[Abstract](#)[Introduction](#)[Conclusions](#)[References](#)[Tables](#)[Figures](#)[Back](#)[Close](#)[Full Screen / Esc](#)[Printer-friendly Version](#)[Interactive Discussion](#)

amplitude variations are observed such as between 1479 and 1565 and between 1730 and 1770 with two periods of relatively warmer and wetter winters. Between 1610 and 1730 a period of relatively cooler and dryer winters occurs and may relate to a decrease in solar irradiance during the Maunder Minimum (1640–1714). Seasonal  $\delta^{18}\text{O}$  variations indicate a  $2.5^\circ\text{C}$  seasonality in cave air temperature during the two periods with warmer and wetter winters (1479–1565 and 1730–1770), and correspond to the cave air temperature seasonality observed today. a smaller  $1.5^\circ\text{C}$  seasonality in cave air temperature occurs during the interval with colder and wetter winters between 1610 and 1730 and suggests colder summers. The  $\delta^{13}\text{C}$  seasonal changes suggest that the seasonality in discharge was lower than the one observed today with a short interval of increased seasonality between 1600 and 1660 reflecting stronger summer PCP-effects due to decreased winter recharge.

## 1 Introduction

Climate reconstructions such as the Northern Hemisphere temperature curve (Mann et al., 1999) or the NAO variation curve (Trouet et al., 2009) are based on a selection of climate archives such as tree-rings, ice-cores, speleothems or lake sediments. To refine these curves and obtain more regionally relevant information, more detailed and better regionally spread climate proxy reconstructions at yearly or even seasonal resolution are necessary. In the studied western European region, high-resolution proxy climate records covering the last 500 years are scarce. Most climate information at seasonal or yearly scale is retrieved from historical data such as the price of flour or grapes (Van Engelen et al., 2001; Le Roy Ladurie, 2004) which may induce biases in the climate record. Therefore it is necessary to confront information from different archives, based on different approaches.

Speleothems have already often proven to enable climate reconstruction at high-resolution in Europe (Genty et al., 2003; Baker et al., 2011; McDermott et al., 2011; Fohlmeister et al., 2012; Verheyden et al., 2014). On multimillennial and centennial

scales, the  $\delta^{18}\text{O}$  and  $\delta^{13}\text{C}$  variations can often be related to a single climate proxy such as temperature or vegetation cover (Spotl and Mangini, 2002; Genty et al., 2003; McDermott, 2005). However, on decadal and seasonal scale, a larger range of factors can influence the  $\delta^{18}\text{O}$ ,  $\delta^{13}\text{C}$ , layer thickness or calcite fabric of a speleothem making an interpretation in terms of climate more difficult. To allow reconstructing the climate up to seasonal variation using mid-latitude speleothems, a detailed analysis of each used proxy must be compared with a multiproxy approach. Different European records have enabled to reconstruct climate successfully by using this approach (Frisia et al., 2003; Niggemann et al., 2003; Mangini et al., 2005; Matthey et al., 2008; Fohlmeister et al., 2012).

Belgian speleothems have the valuable advantage to often display a clear internal layered structure reflecting seasonal variations (Genty and Quinif, 1996). The link between layer thickness and water excess in Belgian stalagmites for the Late Glacial and Holocene period has clearly been demonstrated by Genty and Quinif (1996). The  $\delta^{18}\text{O}$  and  $\delta^{13}\text{C}$  signals from a speleothem sampled in the Pèrè Noël cave were interpreted as due to variations in cave humidity and drip rate inducing changes in the kinetics of the calcite deposition occurring closer or less close to isotopic equilibrium. More negative  $\delta^{18}\text{O}$  and  $\delta^{13}\text{C}$  values occur during periods of higher cave water recharge, when calcite deposition occurs closer to isotopic equilibrium (Verheyden et al., 2008). In this speleothem, the isotopic ( $\delta^{18}\text{O}$  and  $\delta^{13}\text{C}$ ) and geochemical (Mg/Ca and Sr/Ca) proxies vary similarly and record the climate in terms of wetter and dryer phases (Verheyden et al., 2014). The studied Proserpine stalagmite is a large tabular shaped speleothem, growing in the Han-sur-Lesse cave, which is part of the same cave system as the Pèrè Noël cave. A former study of the stalagmite revealed deposition from 200 to 2001 AD, indicating an exceptionally high average growth rate of  $\pm 1 \text{ mm yr}^{-1}$ . The upper 60 cm, which covers the last 500 years is clearly layered (Verheyden et al., 2006). The similar variability of the  $\delta^{18}\text{O}$  and  $\delta^{13}\text{C}$  signals and the layer thickness was linked to changes in effective precipitation (rainfall minus evapo-transpiration) (Verheyden et al., 2006).

CPD

10, 4149–4190, 2014

## A 500 year seasonally resolved $\delta^{18}\text{O}/\delta^{13}\text{C}$

M. Van Rampelbergh  
et al.

Title Page

Abstract

Introduction

Conclusions

References

Tables

Figures



Back

Close

Full Screen / Esc

Printer-friendly Version

Interactive Discussion



These proxies therefore have the potential to be used to reconstruct climate in terms of wetter and dryer phases.

In this paper we study this potential more in detail and up to a seasonally resolved timescale. An absolute age model is established by combining layer-counting ages with measured U/Th-ages. A comparison of variations in layer thickness, calcite fabric,  $\delta^{18}\text{O}$  and  $\delta^{13}\text{C}$  signals in the light of former studies (Genty and Quinif, 1996; Verheyden, 2001; Genty et al., 2003; Mühlinghaus et al., 2007; Wackerbarth et al., 2010; Fohlmeister et al., 2012; Verheyden et al., 2014) and monitoring of the same stalagmite location (Van Rampelbergh et al., 2014) leads to a better understanding of how these proxies are related among them as well as with the monitoring data, and how they reflect climate variations. The derived climate interpretation is further verified and refined by comparing the Proserpine climate signal with temperature reconstructions in the Northern Hemisphere (Jones and Mann, 2004) and Europe (Van Engelen et al., 2001; Le Roy Ladurie, 2004; Luterbacher et al., 2004; Dobrovolny et al., 2010) as well as with a winter NAO reconstruction (Trouet et al., 2009).

## 2 Study area

The Proserpine stalagmite is sampled in the Salle-du-Dôme chamber in the Han-sur-Lesse cave, southern Belgium (Fig. 1). The Han-sur-Lesse cave is a meander cutting of the Lesse-river, which still flows through the cave. The large rooms, the multiple entrances and the presence of the river make it a well-ventilated cave. Part of the cave, including the Salle-du-Dôme, is a show cave since the mid 19th century. The Salle-du-Dôme, being the largest chamber of the cave system (150 m wide and 60 m high), is located under ca. 40 m of Givetian limestone (Quinif, 1988) with a C3-type vegetation covered soil. The Proserpine stalagmite is a 2 m high stalagmite with a large tabular shape (with a horizontal 70 cm by 150 cm to surface) that was actively growing when cored in 2001. A rain of seepage water throughout the year feeds the stalagmite. Such

CPD

10, 4149–4190, 2014

## A 500 year seasonally resolved $\delta^{18}\text{O}/\delta^{13}\text{C}$

M. Van Rampelbergh et al.

Title Page

Abstract

Introduction

Conclusions

References

Tables

Figures



Back

Close

Full Screen / Esc

Printer-friendly Version

Interactive Discussion



fast growing “tam-tam” shaped stalagmites have the property to record climate signals and environmental information at high resolution (Perette, 2000).

The mean annual precipitation at the nearest meteorological station of Han-sur-Lesse is  $844 \text{ mm yr}^{-1}$  and the mean annual air temperature averages  $10.3^\circ\text{C}$  (Royal Meteorological Institute Belgium) characterizing a warm temperate, fully humid climate with cool summers (Kottek et al., 2006). While the temperature displays a well-marked seasonality with cool summers and mild winters, the rainfall is spread all over the entire year. The external seasonality in temperature causes a subdued temperature variation within the Salle-du-Dôme of  $2$  to  $2.5^\circ\text{C}$  between summer and winter (Van Rampelbergh et al., 2014). During summer the stronger evapotranspiration causes the drip discharge to diminish. Both isotopic signals ( $\delta^{18}\text{O}$  and  $\delta^{13}\text{C}$ ) are interpreted to be deposited in equilibrium under the present-day conditions (Van Rampelbergh et al., 2014). The  $\delta^{18}\text{O}$  signal of freshly formed calcite collected on top of the Proserpine varies seasonally due the changes in cave air temperature. The  $\delta^{13}\text{C}$  signal varies seasonally due to changes in prior calcite precipitation intensity, driven by changes in net precipitation (Van Rampelbergh et al., 2014).

### 3 Methods

The Proserpine stalagmite was sampled in January 2001, by drilling a 2 m core in the tabular shaped stalagmite. The precise location was on the side with the highest drip rate but far enough away from the edge to avoid disturbance of the expected horizontal layering of the growth increments (Fig. 1b). The core was cut in half and a slab of 1 cm was cut from the center. The slabs were polished by hand with carbide powder and finished with  $\text{Al}_2\text{O}_3$ . The upper 56 cm, was further studied and cut in seven parts, numbered I to VII (Fig. 2), to allow easy handling in the laboratory. A petrographic description was done and layers were counted per part, under the Mercantec Micromill microscope and on high-resolution scans using Adobe Illustrator. To increase the reliability of the layer counting, layers were counted by different authors, on different days

## A 500 year seasonally resolved $\delta^{18}\text{O}/\delta^{13}\text{C}$

M. Van Rampelbergh et al.

Title Page

Abstract

Introduction

Conclusions

References

Tables

Figures



Back

Close

Full Screen / Esc

Printer-friendly Version

Interactive Discussion







0.3 mm layer<sup>-1</sup>. In the parts II to IV layer thickness increases to 0.5 mm layer<sup>-1</sup> with very clear easily countable layering in part IV. In the parts V to VII layer thickness averages 1 mm layer<sup>-1</sup> with well distinguishable layers in part VII. Superimposed short intervals of darker, more compact and thinner layers of 0.2 mm layer<sup>-1</sup> occur between 7 and 8 cm and between 34 and 36 cm.

## 4.2 U/Th and layer counting ages

Eight U/Th-ages that were previously published by some of us (Verheyden et al., 2006) are used and numbered 1, 2, 7, 8, 15, 17, 18 and 19, and marked in light grey in Table 1. Twelve new U/Th ages measured in this study are listed in black in Table 1 and correspond well with the previously measured ages. Due to the large amounts of detrital <sup>232</sup>Th, the U/Th-ages of samples from part I have large error bars. For each part, the amount of years obtained by StalAge, as well as by layer counting are listed in Table 2, together with their suggested growth rate. With the exception of part IV, both independent approaches deliver similar results within their uncertainty ranges. The uncertainties obtained by layer counting are substantially smaller than the ones obtained by StalAge (Table 2). The growth rates per part, based on layer counting, are low at 0.6 mm yr<sup>-1</sup> in part I, higher around 1 mm yr<sup>-1</sup> in part II, III and IV, and very high at 2 mm yr<sup>-1</sup> in the parts V, VI, and VII. The growth rates derived by StalAge display much larger variations between the different parts, with exceptionally high growth rates of 5.6 mm yr<sup>-1</sup> for the part IV and 6.5 mm yr<sup>-1</sup> for part VI.

## 4.3 Stable isotopes of oxygen and carbon

The  $\delta^{18}\text{O}$  values average  $-6.6 \pm 0.16\text{‰}$  in part I and are slightly more negative in the parts II to VII with an average of  $-7.0 \pm 0.12\text{‰}$  (Fig. 3). The  $\delta^{13}\text{C}$  values average  $-10 \pm 0.12\text{‰}$ , with no significant difference between part I and the parts II to VII. The  $\delta^{18}\text{O}$  and  $\delta^{13}\text{C}$  signals are well correlated ( $R^2 = 0.64$ ) between the top and 12.5 cm (in part I and in the heavily altered and more matte upper section of part II). A much lower

CPD

10, 4149–4190, 2014

## A 500 year seasonally resolved $\delta^{18}\text{O}/\delta^{13}\text{C}$

M. Van Rampelbergh  
et al.

Title Page

Abstract

Introduction

Conclusions

References

Tables

Figures



Back

Close

Full Screen / Esc

Printer-friendly Version

Interactive Discussion



**A 500 year seasonally resolved  $\delta^{18}\text{O}/\delta^{13}\text{C}$** M. Van Rampelbergh  
et al.

Title Page

Abstract

Introduction

Conclusions

References

Tables

Figures



Back

Close

Full Screen / Esc

Printer-friendly Version

Interactive Discussion



correlation coefficient is calculated between 12.5 and 56 cm (parts II to VII) ( $R^2 = 0.16$ ). In the latter part both isotopic signals display different long-term variations. The  $\delta^{18}\text{O}$  signals display two periods with more negative values varying around  $-7.5 \pm 0.16\%$  between 14 and 18.5 cm and between 38 and 56 cm. From 18.5 to 38 cm, in between the two more negative periods, the  $\delta^{18}\text{O}$  values are higher and vary around  $-6.8 \pm 0.16\%$ . No such variations are visible in the  $\delta^{13}\text{C}$  values. They remain more stable around  $-10 \pm 0.12\%$ . Superimposed on the above discussed variations, four shorter-term, large amplitude shifts, occur between 7 and 8 cm, between 11 and 12.5 cm, at 18.5 cm and between 32 and 38 cm. Isotopic values display a simultaneous increase up to  $-6.0 \pm 0.16\%$  for the  $\delta^{18}\text{O}$  and to  $-8.0 \pm 0.12\%$  for the  $\delta^{13}\text{C}$  values.

In the parts II to VII, the layering is clearly visible and the sampling resolution is seasonal being one sample per layer. The  $\delta^{18}\text{O}$  and  $\delta^{13}\text{C}$  signals demonstrate very clear seasonal (Fig. 3) variations superimposed on the variations described above. The seasonality is defined as the amplitude of the seasonal variations, which is the difference in proxy values between darker and whiter layers. The seasonality in  $\delta^{18}\text{O}$  is stronger during the two more negative periods, between 14 and 18.5 cm and between 38 and 56 cm, and equals 0.5‰. Between 18.5 and 32 cm, the  $\delta^{18}\text{O}$  seasonality lowers to 0.25‰. For  $\delta^{13}\text{C}$ , the seasonality averages at 0.7‰. An increase in  $\delta^{13}\text{C}$  seasonality to 1.5‰ occurs at 32 cm and is followed by a gradual decrease until 27 cm when the seasonality returns to 0.7‰.

## 5 Discussion

### 5.1 Speleothem Age model

Two independent geochronological methods were used to establish the age model of the Proserpine: StalAge based on 20 U/Th-ages and layer counting. The total amount of years for the studied part of the Proserpine corresponds for both methods. However, when compared in more detail, part per part, the ages obtained by StalAge do not

**A 500 year seasonally resolved  $\delta^{18}\text{O}/\delta^{13}\text{C}$** M. Van Rampelbergh  
et al.[Title Page](#)[Abstract](#)[Introduction](#)[Conclusions](#)[References](#)[Tables](#)[Figures](#)[Back](#)[Close](#)[Full Screen / Esc](#)[Printer-friendly Version](#)[Interactive Discussion](#)

always correspond with the ages derived from counting the yearly layer couplets. Such is the case for part IV where StalAge suggests the part was deposited in  $19 \pm 46$  years while the layer counting indicates a total of  $105 \pm 11$  layer couplets (Table 2). The very clear layering in part IV makes it highly improbable that too many layers have been counted. Furthermore, the uncertainty on the reported StalAge age for part IV is larger than the modeled value itself, indicating the very large uncertainty of the StalAge model in that part. This is due the five consecutive U/Th-ages;  $1676 \pm 71$  AD,  $1634 \pm 30$  AD,  $1617 \pm 30$  AD,  $1635 \pm 26$  AD and  $1637 \pm 17$  AD that cover the segment between 19.5 and 34.2 cm and all suggest an age of  $\sim 1600$  within their error range. These similar ages for a large part of the stalagmite cause the StalAge modeled growth rate in part IV to increase to unrealistically high values of  $5.9 \text{ mm yr}^{-1}$ . Speleothems growing in cool temperate climate have growth rates varying between 0.01 and  $0.1 \text{ mm yr}^{-1}$  (Fairchild et al., 2006) indicating that the StalAge suggested growth rate is very improbable. The growth rate obtained by layer counting equals  $1.1 \text{ mm layer}^{-1}$  in part IV, being still high but more within the expected rates for the fast growing Proserpine. A similar problem occurs in part VI. The StalAge model suggests an exceptionally high growth rate of  $6.5 \text{ mm yr}^{-1}$  for part VI while the layer counting ages results in a growth rate of  $2.1 \text{ mm yr}^{-1}$ , still very high, but acceptable for the fast growing Proserpine stalagmite (Verheyden et al., 2006).

Layer thickness measurements indicate thinnest layers of on average 0.3 mm in part I, thicker layers of 0.5 mm in part II, III and IV and exceptionally large layers well over 1 mm in parts V, VI and VII. Two phases in which the growth rate noticeably increases may be expected at the transition of part I in part II and at the transition of part IV in V. Such a growth rate increase at the transition of part I in part II and at the transition of part IV in V is suggested in the layer counting growth rates while the StalAge growth rates do not display a growth rate change at these points (Table 2).

The more realistic growth rates suggested by the layer counting age model and the good agreement between the changes in growth rates suggested by the layer counting model and the changes in growth rate indicated by the layer thickness measurements

suggests that the layer counting age model is the most accurate. The layer counting age model is thus used to establish the chronology of the Proserpine.

Based on the layer counting ages, the bottom of part I is estimated at  $1847 \pm 10$  AD. Below the perturbation (at 10 cm), an age estimation of the onset of the perturbation has to be made to restart the layer counting ages downwards. A first possible way to estimate this age is to count the layers back upward from the U/Th-age located closest below the perturbation ( $= 1798 \pm 45$  AD). By doing this, the counted age for the top layer of part II is  $1810 \pm 51$  AD. A second possible way is to use the StalAge modeled age of  $1810 \pm 48$  AD for the top of part II. Both age-estimations are in excellent agreement. A  $^{14}\text{C}$ -date on a straw piece embedded in the perturbed calcite indicates an age interval of 1760 to 1810 (Verheyden et al., 2006) also suggesting a similar time window for the perturbation. The age of  $1810 \pm 48$  AD modeled by StalAge, has the smallest age uncertainty of all three methods and is based on a statistical combination of the measured U/Th-dates before and after the modeled age (Scholz and Hoffmann, 2011). This age is thus considered more robust than the layer counted age based on solely one U/Th-age point, and is the one we use for the onset of the perturbation. Based on this age of  $1810 \pm 48$  AD, and with  $331 \pm 65$  layer couplets counted in the parts II to VII, an age of  $1479 \pm 113$  AD is suggested for the start of the record at 56 cm.

## 5.2 Variations in $\delta^{18}\text{O}$ , $\delta^{13}\text{C}$ , layer thickness and calcite fabric

Cave monitoring results show that fresh-farmed Proserpine calcite is deposited in equilibrium with the drip water. The  $\delta^{18}\text{O}$  values vary seasonally between  $-6.5 \pm 0.15\%$  and  $-7.0 \pm 0.12\%$  and the  $\delta^{13}\text{C}$  values vary seasonally between  $-10 \pm 0.12\%$  and  $-11 \pm 0.12\%$  (Van Rampelbergh et al., 2014). Between 1565 and 1610, at 1730, between 1770 and 1800 and between 1880 and 1895, the  $\delta^{18}\text{O}$  and  $\delta^{13}\text{C}$  values measured in the Proserpine shift to values up to  $-6.0 \pm 0.16\%$  for  $\delta^{18}\text{O}$  and  $-8.0 \pm 0.12\%$  for  $\delta^{13}\text{C}$  indicating that calcite is not deposited in equilibrium with the drip water. During these disequilibrium periods, layer thickness and calcite fabric display large-scale

CPD

10, 4149–4190, 2014

## A 500 year seasonally resolved $\delta^{18}\text{O}/\delta^{13}\text{C}$

M. Van Rampelbergh  
et al.

Title Page

Abstract

Introduction

Conclusions

References

Tables

Figures



Back

Close

Full Screen / Esc

Printer-friendly Version

Interactive Discussion





ative and layers are thicker. Between 1610 and 1730, when  $\delta^{18}\text{O}$  values are less negative and layers are thinner, the seasonal amplitude lowers to 0.25‰. The  $\delta^{13}\text{C}$  seasonality mostly equals 0.7‰ with a superimposed period where it increases to 1.5‰ at 1600 followed by a gradual return to 0.7‰ around 1660.

### 5.3 Possible factors driving the $\delta^{18}\text{O}$ and $\delta^{13}\text{C}$ values, layer thickness and calcite fabric

Variations in speleothem  $\delta^{18}\text{O}$  values deposited in equilibrium can relate to changes in temperature, rainfall amount or source of the rainfall (Fairchild et al., 2006). Rainfall sources often imply  $\delta^{18}\text{O}$  shifts in the order of several ‰ (Fleitmann et al., 2007) while the  $\delta^{13}\text{C}$  values and layer thickness values remain unchanged. The large-scale  $\delta^{18}\text{O}$  variations in the Proserpine are in the order of 1 to 2‰ and always occur together with large-scale  $\delta^{13}\text{C}$  variations of the same order and a decrease in layer thickness indicating that the source effect is most probably not responsible for these  $\delta^{18}\text{O}$  variations. Due to the “amount-effect” (Dansgaard, 1964) increased rainfall amounts can cause the speleothem  $\delta^{18}\text{O}$  values to increase during wetter periods, which is often observed in tropical and sub-tropical speleothem  $\delta^{18}\text{O}$  signals (Fleitmann et al., 2007; Wang et al., 2008). Comparison between the Proserpine  $\delta^{18}\text{O}$  and the annual precipitation amounts measured by the Royal Meteorological Institute (RMI) in Belgium since 1833 display no link indicating that rainfall amounts are not the primary driver of the  $\delta^{18}\text{O}$  variations (Fig. 5a and e). Temperature changes can also affect the speleothem  $\delta^{18}\text{O}$  value and are more commonly expected in mid-latitude temperate climates. Multimillennial large-scaled temperature variations such as Dansgaard/Oeschger cycles cause European speleothem  $\delta^{18}\text{O}$  values to decrease with decreasing temperature (Spotl and Mangini, 2002; Genty et al., 2003). Large amplitude climatic events such as the 8.2 kyr cold event are also clearly recorded in European speleothems mostly as a decrease in  $\delta^{18}\text{O}$  values (Baldini et al., 2002; Fohlmeister et al., 2012; Verheyden et al., 2014). However, smaller scaled temperature variations are more difficultly recorded in

## A 500 year seasonally resolved $\delta^{18}\text{O}/\delta^{13}\text{C}$

M. Van Rampelbergh  
et al.

Title Page

Abstract

Introduction

Conclusions

References

Tables

Figures



Back

Close

Full Screen / Esc

Printer-friendly Version

Interactive Discussion



**A 500 year seasonally resolved  $\delta^{18}\text{O}/\delta^{13}\text{C}$** M. Van Rampelbergh  
et al.

Title Page

Abstract

Introduction

Conclusions

References

Tables

Figures



Back

Close

Full Screen / Esc

Printer-friendly Version

Interactive Discussion



speleothems and can cause the  $\delta^{18}\text{O}$  signal to increase or decrease with decreasing temperature. The reason for this is that the temperature effect on the rainwater  $\delta^{18}\text{O}$  is opposite to the temperature effect on calcite deposition. The temperature effect on the rainwater  $\delta^{18}\text{O}$  signal can vary between  $0.17$  and  $0.9\text{‰}\text{°C}^{-1}$ , depending on the geographical location (Dansgaard, 1964; Rozanski et al., 1992; Mook, 2000; Schmidt et al., 2007). Schmidt et al. (2007) suggested a dependence of  $0.3\text{‰}\text{°C}^{-1}$  for central Europe. The temperature dependent fractionation during calcite formation within the cave acts in the opposite direction, and is around  $-0.2\text{‰}\text{°C}^{-1}$  for the Proserpine drip site as suggested by monitoring results (Van Rampelbergh et al., 2014). The net effect for the Proserpine would thus be  $0.1\text{‰}\text{°C}^{-1}$  considering that the  $0.3\text{‰}\text{°C}^{-1}$  temperature dependence of the rainwater is also valid for Belgium. The uncertain link between the Proserpine  $\delta^{18}\text{O}$  values and the annual temperature is further indicated by the absence of a correlation with annual temperatures measured by the Belgian RMI since 1833. We therefore do not a priori expect the  $\delta^{18}\text{O}$  variations measured in the Proserpine to be related to solely yearly temperature nor to solely yearly rainfall variations.

Previous studies of western European Holocene speleothems growing in a similar climate as the Han-sur-Lesse cave, have shown that speleothem  $\delta^{18}\text{O}$  values relate to winter temperatures and winter precipitation intensities rather than to yearly temperature and precipitation intensities (Mangini et al., 2005; Wackerbarth et al., 2010; Fohlmeister et al., 2012). Hydrological studies of the Han-sur-Lesse epikarst show that the epikarst recharge mostly occurs between spring and fall with largest amounts of recharge in winter (Bonniver, 2011). Winter rainfall has a lower isotopic composition compared to the rainfall from other seasons. Consequently, during periods of lower winter recharge, less isotopically light water will be added to the epikarst reservoir and the total  $\delta^{18}\text{O}$  composition of the epikarst water will increase, causing increased  $\delta^{18}\text{O}$  values in the speleothem. Furthermore, lower winter precipitation intensities (DJF) correlate ( $R^2 = 0.23$ ) with lower winter temperatures (DJF) measured by the Belgian RMI since 1833. Colder winters are consequently drier winters. Increased speleothem  $\delta^{18}\text{O}$  values are consequently interpreted to relate with colder and drier winters. A similar re-

lation between  $\delta^{18}\text{O}$  and winter temperature and precipitation has been observed at a German growth site with similar climatic conditions as the Proserpine growth site (Wackerbarth et al., 2010; Fohlmeister et al., 2012).

When deposited in equilibrium, large scaled  $\delta^{13}\text{C}$  variations may relate to vegetation type changes above the cave (C3 or C4-vegetation). Such changes may induce  $\delta^{13}\text{C}$  shifts of 8 to 10‰ (Cerling, 1984). However, the actual C3-vegetation is the normal natural flora of the environment and there are no indications of anthropogenic impact or other dramatic environmental changes that would have possibly led to substantial changes in the C3/C4-ratio. With no major vegetation changes and calcite being deposited in equilibrium with the drip water, lower  $\delta^{13}\text{C}$  values in temperate regions are often related to an increase of soil activity, mainly occurring during warmer and humid conditions (Genty et al., 2003; Fohlmeister et al., 2012). Plant- $\text{CO}_2$  has a lower isotopic signature compared to atmospheric  $\text{CO}_2$  ( $\delta^{13}\text{C}$  of C3-vegetation is between  $-20$  and  $-25$ ‰, while in atmospheric  $\text{CO}_2$  it evolved from  $-7$  to  $-8$ ‰ during the studied period). A reduced plant- $\text{CO}_2$  input in the soil will increase the  $\delta^{13}\text{C}$  of the soil- $\text{CO}_2$  reservoir and consequently the dissolved inorganic carbon (DIC) in the epikarst water. However, changes in soil activity are relatively slow and expected to cause more gradual long-term  $\delta^{13}\text{C}$  variations. The  $\delta^{13}\text{C}$  variations in the Proserpine a short-scaled (centennial and decadal) and more abrupt variations and are consequently not expected to be driven by changes in soil activity.

Processes with a faster reaction time such as for example prior calcite precipitation (PCP) or disequilibrium processes are more likely to be responsible for the observed  $\delta^{13}\text{C}$  variations. During PCP, calcite is deposited from the percolating epikarst water before entering the cave as drip water. This process mostly occurs during drier periods when aerated zones become more important in the epikarst. PCP causes a simultaneous increase in the  $\delta^{13}\text{C}$  and in the Mg/Ca and Sr/Ca composition of the drip water and speleothem calcite (Fairchild et al., 2000). Although no Mg/Ca and Sr/Ca ratios are measured in the Proserpine, which makes it difficult to evaluate the process of PCP, monitoring results have clearly demonstrated that PCP is present in the Han-sur-Lesse

## A 500 year seasonally resolved $\delta^{18}\text{O}/\delta^{13}\text{C}$

M. Van Rampelbergh  
et al.

[Title Page](#)[Abstract](#)[Introduction](#)[Conclusions](#)[References](#)[Tables](#)[Figures](#)[Back](#)[Close](#)[Full Screen / Esc](#)[Printer-friendly Version](#)[Interactive Discussion](#)



## A 500 year seasonally resolved $\delta^{18}\text{O}/\delta^{13}\text{C}$

M. Van Rampelbergh  
et al.

Title Page

Abstract

Introduction

Conclusions

References

Tables

Figures



Back

Close

Full Screen / Esc

Printer-friendly Version

Interactive Discussion



is primarily dependent on two factors; the discharge amount and the cave seepage water calcium ion concentration (Genty et al., 2001). Discharge at the Proserpine drip site is expected to lower during drier and colder winters. The second factor, being the amount of calcium ion concentration, depends on (i) the residence time of the water in the epikarst, (ii) soil  $p\text{CO}_2$  and/or on (iii) PCP. If the residence time of the water in the epikarst (i) is longer than several days (Dreybrodt and Scholz, 2011), the water will reach calcite supersaturation. However, since the drip water residence time in the Han-sur-Lesse epikarst is suggested to be longer than one year (Van Rampelbergh et al., 2014), this effect is not expected to cause variations in calcium ion concentration. A higher soil activity increases the soil  $p\text{CO}_2$  (ii) and consequently the amount of  $\text{CO}_2$  dissolved in the water. Water with a higher  $p\text{CO}_2$  more easily dissolves  $\text{CaCO}_3$ , which increases its calcium ion concentration. However, changes in soil activity are considered a slow process causing gradual changes on millennial and multi-millennial scales (Fohlmeister et al., 2012). Soil  $p\text{CO}_2$  variations are consequently not expected to cause decadal and centennial changes in calcium ion concentration. PCP (iii) decreases the  $\text{Ca}^{2+}$  concentration of the drip water due to precipitation of calcite in the epikarst. Cave monitoring results show that PCP is an important process in the Han-sur-Lesse epikarst that becomes more intense during the drier summer season (Van Rampelbergh et al., 2014). PCP is consequently a fast process in the Han-sur-Lesse epikarst and is expected to be responsible for the abrupt decadal and centennial changes in calcium ion concentration in the Proserpine drip water. A decreased calcium ion concentration of the Proserpine drip water is consequently interpreted to occur when recharge is lower during drier and colder winters. The two main factors driving the growth rate, being the drip discharge and the calcium ion concentration, both decrease when recharge is low during drier and colder winter periods. Thinner layers and darker calcite, driven by decreased growth rate, are consequently interpreted to reflect drier and colder winters.

Winter precipitation recharges the Han-sur-Lesse epikarst and a good correlation is present between colder winters and drier winters recorded in instrumental data since



tween 1810 and 1860 is also considered as an anomaly due to the absence of calcite deposition. A total of five anomalies occur in the Proserpine record between 1565 and 1610, at 1730, between 1770 and 1800, between 1810 and 1860 and between 1880 and 1895. More detailed discussion of each anomaly may indicate their forcing and eventual link with climate.

The oldest anomaly lasts from 1565 to 1610 and displays increased  $\delta^{18}\text{O}$  and  $\delta^{13}\text{C}$  values, thinner layers and darker calcite. Detailed analysis of the forcing behind the proxy variations indicate that such simultaneous variations occur when drip discharge shifts under a certain threshold value due to colder and dryer winters. The anomaly between 1565 and 1610 is thus considered as a period with colder and dryer winters. Within this anomaly, a shorter interval with more negative  $\delta^{18}\text{O}$  and  $\delta^{13}\text{C}$  values occurs together with thicker layers between 1590 and 1600 (Fig. 5a–c), indicating a short interval of warmer and wetter winters within the generally cold and dry period from 1565 to 1610. Historical data of France, Belgium and the Netherlands indicate that the period of 1565 to 1610 was characterized by icy cold winters, harsh famines, low numbers of child births and weddings, and by the outbreak of the plague with its worst years from 1562 to 1570 (Le Roy Ladurie, 2004), which confirms our observations. Le Roy Ladurie (2004) interprets the shift to cold and dry conditions at 1565 AD as the onset of the second pulse of the Little Ice Age (LIA). The shorter relatively warmer and wetter interval between 1590 and 1610 is also well-described in historical archives as being a wetter decade (Le Roy Ladurie, 2004). Colder conditions between 1565 and 1610 are also illustrated in proxy based temperature reconstruction from Europe (Fig. 5i) (Luterbacher et al., 2004) and from Central Europe (Fig. 5j) (Dobrovlny et al., 2010). A shift to colder conditions at 1565 is visible in the more general Northern Hemisphere temperature reconstructions, but does not display the return to relatively warmer and wetter conditions at 1610 (Fig. 5f) (Jones and Mann, 2004). The fact that the exceptionally cold and dry interval is only visible in European temperatures and historical records, indicates that it is a regional “European event”, not valid for the whole Northern Hemisphere. Climate variations in western Europe are mostly related to variations

## A 500 year seasonally resolved $\delta^{18}\text{O}/\delta^{13}\text{C}$

M. Van Rampelbergh  
et al.

[Title Page](#)[Abstract](#)[Introduction](#)[Conclusions](#)[References](#)[Tables](#)[Figures](#)[Back](#)[Close](#)[Full Screen / Esc](#)[Printer-friendly Version](#)[Interactive Discussion](#)

**A 500 year seasonally resolved  $\delta^{18}\text{O}/\delta^{13}\text{C}$** M. Van Rampelbergh  
et al.[Title Page](#)[Abstract](#)[Introduction](#)[Conclusions](#)[References](#)[Tables](#)[Figures](#)[Back](#)[Close](#)[Full Screen / Esc](#)[Printer-friendly Version](#)[Interactive Discussion](#)

in the state of the North Atlantic Oscillation (NAO) (Trouet et al., 2009). More negative NAO conditions cause drier conditions over northwestern Europe. Such a negative NAO phase occurred in the period between 1565 and 1610 (Trouet et al., 2009) and may be the cause of the cold and dry winters suggested by the Proserpine (Fig. 5g). A smaller interval with more positive NAO conditions around 1590 may have caused the warmer and wetter interval between 1590 and 1610.

The anomaly at 1730 displays extremely short and abruptly increased isotopic values and thinner layers but does not correspond with darker calcite (Fig. 5a to c). At 1730 layering is strongly disturbed with vertical layers in some parts, which are suggested to relate to rimstone structures on the paleo-surface of the stalagmite. Calcite deposition conditions for such vertically orientated layers may differ from the calcite deposition conditions in horizontal layers. Therefore the observed anomaly may not relate to climate. Comparison with other proxy based climate reconstructions (Van Engelen et al., 2001; Jones and Mann, 2004; Luterbacher et al., 2004; Trouet et al., 2009; Dobrovolny et al., 2010), or historical records (Le Roy Ladurie, 2004) do not suggest a climate variation around 1730 and further indicate that the anomaly at 1730 is most probably not climate-driven. A more detailed study of the evolution of the isotopes along the layers in this part together with thin section analyses may provide better insights in the processes affecting the  $\delta^{18}\text{O}$  and  $\delta^{13}\text{C}$  and layer thickness values around 1730.

The anomaly between 1770 and 1800 displays increased isotopic values and decreased layer thickness followed by a very abrupt shift back to more negative isotopic values and larger layers at 1800. The calcite fabric is very matte white and may possibly be altered by non-climatic factors. For example, the heat of fires lit on the surface of the stalagmite between 1810 and 1860 may have altered the proxy signals. However, the increased isotope values and thinner layers may not fully be overprinted by the alteration and still reflect colder and dryer winter conditions. This observation corresponds with colder conditions in Europe (Fig. 5h–j) (Van Engelen et al., 2001; Le Roy Ladurie, 2004; Luterbacher et al., 2004; Dobrovolny et al., 2010) and confirms, that although calcite is white matte, the isotopes still record climate variations. However, no colder

interval is visible in the Northern Hemisphere (Jones and Mann, 2004) suggesting that the cooling was most probably local to Europe rather than to whole Northern Hemisphere. A decreased NAO index (Trouet et al., 2009) could possibly be the driver of this colder and dryer winter interval in Europe.

Between 1810 and 1860, straw pieces are found embedded in the calcite crust and suggest that fires were lit on the surface of the stalagmite to illuminate the chamber (Verheyden et al., 2006). Fires could only be lit on the Proserpine under the absence of drip water and indicate exceptionally dry conditions. Historical climate data from France, Belgium and the Netherlands indicates that the period between 1800 and 1860 is the last cold pulse of the Little Ice Age (LIA,  $\pm 1300$ –1850) and is characterized by exceptionally cold winters followed by warm summers (Le Roy Ladurie, 2004). The consequence of harsh winters followed by warm summers may have added to the general discontent in France that led to the onset of the French Revolution in 1789 (Mann, 2002). The warm summers and cold winters cause no significant temperature drop in the yearly average temperature reconstructions from Europe, Central Europe or the Northern Netherlands (Fig. 5h–j) (Van Engelen et al., 2001; Luterbacher et al., 2004; Dobrovolny et al., 2010). However, the colder and dryer LIA pulse is well registered by a temperature drop in the Northern Hemisphere temperatures (Jones and Mann, 2004) (Fig. 5f). Between 1810 and 1860 winter NAO conditions shifted to negative values, which may have caused the exceptionally dry winter conditions recorded in the Proserpine (Fig. 5g) (Trouet et al., 2009). A decrease in solar irradiance occurs between 1790 and 1830, referred as the Dalton Minimum, may also be responsible for this cold and dry period (Mann, 2002). Other climate reconstructions indicate that this cold and dry interval relates to the increased volcanic eruptions during that period (Wagner and Zorita, 2005). A prominent example is the 1815 eruption of the Tambora in Indonesia that injected a large amount of sunlight-reflecting aerosols in the atmosphere and that is typically blamed for the following cold summer years (Mann, 2002).

The most recent anomaly occurs between 1895 and 1880 with increased  $\delta^{18}\text{O}$  and  $\delta^{13}\text{C}$  signals, thinner layers and darker calcite. The colder and dryer winter conditions

CPD

10, 4149–4190, 2014

## A 500 year seasonally resolved $\delta^{18}\text{O}/\delta^{13}\text{C}$

M. Van Rampelbergh  
et al.

Title Page

Abstract

Introduction

Conclusions

References

Tables

Figures



Back

Close

Full Screen / Esc

Printer-friendly Version

Interactive Discussion





## A 500 year seasonally resolved $\delta^{18}\text{O}/\delta^{13}\text{C}$

M. Van Rampelbergh  
et al.

Title Page

Abstract

Introduction

Conclusions

References

Tables

Figures



Back

Close

Full Screen / Esc

Printer-friendly Version

Interactive Discussion



with the layer thickness values suggests an evolution to warmer and wetter winters up to 1930 followed by an evolution to colder and dryer winters to 2001. This observation in the Proserpine proxies does not correspond with climate variations in the Northern Hemisphere (Van Engelen et al., 2001; Jones and Mann, 2004; Le Roy Ladurie, 2004; Luterbacher et al., 2004; Dobrovolny et al., 2010) or with instrumental RMI data since 1833. Calcite is darker in this part due to the incorporation of soot from torches used to illuminate the chamber during cave visits (Verheyden et al., 2006). Soot incorporation in the calcite structure may hamper the calcite deposition and overprint lower-amplitude climate variations. However, large-amplitude climate variations (= anomalies) such as the cold and dry period between 1880 and 1895 are still visible within this part, indicating that the climate signal is not fully overprinted. The possible effects of soot on  $\delta^{18}\text{O}$  and  $\delta^{13}\text{C}$  values and layer thickness need further investigation to allow deriving low-amplitude climate variations.

Below the perturbation a small interval of very negative  $\delta^{18}\text{O}$  and  $\delta^{13}\text{C}$  values occurs between 1800 and 1810. This short interval consists of strongly disturbed calcite in the form of a crust, with no layering visible. Most probably, the heat of fires lit on the Proserpine between 1810 and 1860 (Verheyden et al., 2006) caused the calcite to develop this crust structure. Isotope values are interpreted strongly disturbed and are not used to reconstruct climate variations. With the exception of this calcite crust, the  $\delta^{18}\text{O}$  and layer thickness signals below the perturbation can be subdivided in three periods; between 1479 and 1565, between 1610 and 1730 and between 1730 and 1770 (Fig. 5a and b). Between 1479 and 1565 and between 1730 and 1770,  $\delta^{18}\text{O}$  values vary around  $-7.5 \pm 0.16\text{‰}$  and layer thickness is larger than  $0.8 \text{ mm layer}^{-1}$ . The period between 1610 and 1730, falls in between the two latter periods and displays less negative  $\delta^{18}\text{O}$  values around  $-6.8 \pm 0.12\text{‰}$  and thinner layers around  $0.4 \text{ mm layer}^{-1}$ . The more negative  $\delta^{18}\text{O}$  values and thicker layers in the two periods between 1479 and 1565 and between 1730 and 1770 are interpreted to reflect wetter and warmer winters. The less negative  $\delta^{18}\text{O}$  values and thinner layers between 1610 and 1730 indicate that winters were cooler and dryer compared to the two periods between 1579

## A 500 year seasonally resolved $\delta^{18}\text{O}/\delta^{13}\text{C}$

M. Van Rampelbergh  
et al.

Title Page

Abstract

Introduction

Conclusions

References

Tables

Figures



Back

Close

Full Screen / Esc

Printer-friendly Version

Interactive Discussion



and 1565 and between 173 and 1770 were winters were warmer and wetter. During the three above described periods (1479–1565, 1610–1730, 1730–1770), the  $\delta^{13}\text{C}$  values vary mostly around  $-10 \pm 0.12\text{‰}$  indicating no major changes in PCP intensity. However, during the period with colder and drier winters between 1610 and 1730, the  $\delta^{13}\text{C}$  display a weak gradual increase from 1700 to 1730. The dry and cool winter conditions in the period between 1610 and 1730 may have started to cause a gradual increase in prior calcite precipitation, which gradually increased the  $\delta^{13}\text{C}$  signal.

The two periods with warmer and wetter winters (1479–1565 and 1730–1770) correspond with two clear periods of warmer Northern Hemisphere temperatures (Jones and Mann, 2004) (Fig. 5f). These two warmer pulses are also well documented in historical records and indicated as two warmer intervals during the LIA (Le Roy Ladurie, 2004). The period with cooler and drier winters between 1610 and 1730 corresponds with decreased Northern Hemisphere temperatures. No major winter NAO changes occur during the three periods (1479–1565, 1610–1730, 1730–1770), indicating that the variations are not driven by NAO, most probably by more global climate forcing mechanisms. The colder interval between 1610 and 1730 may be related to the Maunder Minimum, being a period of decreased solar activity between 1640 and 1714. The Maunder Minimum is interpreted to have caused lower temperatures in Europe (Luterbacher et al., 2001) and is also interpreted to be the cause of a similar colder interval in Italian speleothems (Frisia et al., 2003).

### 5.6 Seasonality in $\delta^{18}\text{O}$ and $\delta^{13}\text{C}$ values

The  $\delta^{18}\text{O}$  and  $\delta^{13}\text{C}$  values were measure at a seasonal scale between 1479 and 1810 and clearly display seasonal variations (Fig. 5). Cave monitoring results show that under present-day conditions, the  $\delta^{18}\text{O}$  values display a seasonality of  $0.5\text{‰}$  in response to the seasonality in cave air temperature and has a temperature dependence of  $-0.2\text{‰}\cdot\text{C}^{-1}$  (Van Rampelbergh et al., 2014). The seasonality in  $\delta^{18}\text{O}$  measured in the Proserpine is larger during the two periods with wetter and warmer winters between 1479 and 1565 and between 1730 and 1770 ( $0.5\text{‰}$ ) compared to the period with cooler

**A 500 year seasonally resolved  $\delta^{18}\text{O}/\delta^{13}\text{C}$** M. Van Rampelbergh  
et al.[Title Page](#)[Abstract](#)[Introduction](#)[Conclusions](#)[References](#)[Tables](#)[Figures](#)[Back](#)[Close](#)[Full Screen / Esc](#)[Printer-friendly Version](#)[Interactive Discussion](#)

and dryer winters between 1610 and 1730 (0.25‰). The seasonality in  $\delta^{18}\text{O}$  during the two periods with warmer and wetter winters (1479–1565 and 1730–1770) is similar as the one observed under the present day conditions and corresponds with a 2 to 2.5°C seasonality in cave air temperature. This indicates that temperature seasonality was similar as the one experienced today. During the period with relatively cooler and wetter winters between 1610 and 1730, the  $\delta^{18}\text{O}$  seasonality lowers to 0.25‰ corresponding with a 1 to 1.5°C cave air temperature seasonality. Lower summer temperatures during this cold LIA period are most probably responsible for the lower cave air seasonality.

The  $\delta^{13}\text{C}$  signal mostly displays a seasonality of 0.7‰ being smaller than the 1‰ seasonality in  $\delta^{13}\text{C}$  values observed under the present-day conditions (Van Rampelbergh et al., 2014). At 1600, the  $\delta^{13}\text{C}$  seasonality increases to 1.5‰ and displays a gradual decreasing trend back to 0.7‰ at 1660. Cave monitoring results have indicated that the  $\delta^{13}\text{C}$  seasonality relates to the intensity of PCP, which is increased during the dry summer season. The increase in  $\delta^{13}\text{C}$  seasonality between 1600 and 1660 also corresponds with an interval where layers are thinner ( $\sim 0.4\text{ mm layer}^{-1}$ ) but clearly alternating between dark compact and white porous layers. This suggests well-expressed wet winter conditions and dry summer conditions in the cave. The relatively drier winter conditions in the period between 1610 and 1730 cause the yearly water recharge (occurring in winter) to be lower compared to the two periods with wetter winters between 1479 and 1565 and between 1730 and 1770. A lower recharge during winter will consequently lead to drier cave conditions in summer, and increase the effect of PCP. Increased PCP in summer due to lower winter recharge in the period with colder and drier winters between 1600 and 1730 is interpreted to be responsible for the increased  $\delta^{13}\text{C}$  seasonality and the clear layering between 1600 and 1660.

## 6 Conclusions

1. A multiproxy approach using  $\delta^{18}\text{O}$  and  $\delta^{13}\text{C}$  values, layer thickness and calcite fabric of the Proserpine stalagmite from the Han-sur-Less cave, Belgium, suc-



**A 500 year seasonally resolved  $\delta^{18}\text{O}/\delta^{13}\text{C}$** M. Van Rampelbergh  
et al.

5. Seasonally resolved isotopic signals successfully record seasonal changes in cave air temperature and PCP. The  $\delta^{18}\text{O}$  signals suggest a 2 to 2.5 °C cave air temperature seasonality between 1479 and 1565 and between 1730 and 1770, which is similar to the seasonality in cave air temperature observed today. Between 1610 and 1730, corresponding with a period with cooler and dryer winters, the seasonality in cave air temperature decreases to 1 to 1.5 °C. The  $\delta^{13}\text{C}$  seasonal changes suggest that the seasonality in discharge was lower than observed today with a short interval of increased seasonality between 1600 and 1660 reflecting stronger summer PCP-effects due to decreased winter recharge.

10 *Acknowledgements.* We thank the “Domaine des Grottes de Han” for allowing us to sample the stalagmite and Mr. Van Dierendonck for his interest and support. P. Claeys thanks the Hercules Foundation and Research Foundation (FWO, project G-0422-10).

**References**

- 15 Baker, A., Wilson, R., Fairchild, I. J., Franke, J., Spoetl, C., Matthey, D., Trouet, V., and Fuller, L.: High resolution delta O-18 and delta C-13 records from an annually laminated Scottish stalagmite and relationship with last millennium climate, *Global Planet. Change*, 79, 303–311, 2011.
- Baldini, J. U., McDermott, F., and Fairchild, I. J.: Speleothem trace elements as palaeohydrological proxies during the “8,200 year” cold/dry event, *Geochim. Cosmochim. Ac.*, 66, A46–A46, 2002.
- 20 Bonniver, I.: Etude Hydrogeologique et Dimensionnement par Modelisation du “Systeme-Tracage” du Reseau Karstique the Han-sur-Lesse (Massif de Boine, Belgique), 2011, Geologie, FUNDP Namur, Namur, 93–97, 2011.
- Cerling, T. E.: The stable isotopic composition of modern soil carbonate and its relationship to climate, *Earth Planet. Sc. Lett.*, 71, 229–240, 1984.
- 25 Cheng, H., Edwards, R. L., Hoff, J., Gallup, C. D., Richards, D. A., and Asmerom, Y.: The half-lives of uranium-234 and thorium-230, *Chem. Geol.*, 169, 17–33, 2000.
- Cheng, H., Edwards, R. L., Broecker, W. S., Denton, G. H., Kong, X., Wang, Y., Zhang, R., and Wang, X.: Ice age terminations, *Science*, 326, 248–252, 2009a.

[Title Page](#)[Abstract](#)[Introduction](#)[Conclusions](#)[References](#)[Tables](#)[Figures](#)[Back](#)[Close](#)[Full Screen / Esc](#)[Printer-friendly Version](#)[Interactive Discussion](#)

## A 500 year seasonally resolved $\delta^{18}\text{O}/\delta^{13}\text{C}$

M. Van Rampelbergh  
et al.

Title Page

Abstract

Introduction

Conclusions

References

Tables

Figures



Back

Close

Full Screen / Esc

Printer-friendly Version

Interactive Discussion



Cheng, H., Fleitmann, D., Edwards, R. L., Wang, X. F., Cruz, F. W., Auler, A. S., Mangini, A., Wang, Y. J., Kong, X. G., Burns, S. J., and Matter, A.: Timing and structure of the 8.2 kyr BP event inferred from delta O-18 records of stalagmites from China, Oman, and Brazil, *Geology*, 37, 1007–1010, 2009b.

5 Dansgaard, W.: Stable isotopes in precipitation, *Tellus*, 16, 436–468, 1964.

Deininger, M., Fohlmeister, J., Scholz, D., and Mangini, A.: Isotope disequilibrium effects: the influence of evaporation and ventilation effects on the carbon and oxygen isotope composition of speleothems – a model approach, *Geochim. Cosmochim. Ac.*, 96, 57–79, 2012.

10 Dobrovolny, P., Moberg, A., Brazdil, R., Pfister, C., Glaser, R., Wilson, R., van Engelen, A., Limanowka, D., Kiss, A., Halickova, M., Mackova, J., Riemann, D., Luterbacher, J., and Boehm, R.: Monthly, seasonal and annual temperature reconstructions for Central Europe derived from documentary evidence and instrumental records since AD 1500, *Climatic Change*, 101, 69–107, 2010.

Dreybrodt, W. and Scholz, D.: Climatic dependence of stable carbon and oxygen isotope signals recorded in speleothems: from soil water to speleothem calcite, *Geochim. Cosmochim. Ac.*, 75, 734–752, 2011.

Edwards, R. L., Chen, J. H., and Wasserburg, G. J.:  $^{238}\text{U}$ – $^{234}\text{U}$ – $^{230}\text{Th}$ – $^{232}\text{Th}$  systematics and the precise measurement of time over the past 500 000 years, *Earth Planet. Sc. Lett.*, 81, 175–192, 1987.

20 Fairchild, I. J., Borsato, A., Tooth, A. F., Frisia, S., Hawkesworth, C. J., Huang, Y. M., McDermott, F., and Spiro, B.: Controls on trace element (Sr–Mg) compositions of carbonate cave waters: implications for speleothem climatic records, *Chem. Geol.*, 166, 255–269, 2000.

Fairchild, I. J., Smith, C. L., Baker, A., Fuller, L., Spotl, C., Matthey, D., and McDermott, F.: Modification and preservation of environmental signals in speleothems, *Earth-Sci. Rev.*, 75, 105–153, 2006.

25 Fleitmann, D., Burns, S. J., Mangini, A., Mudelsee, M., Kramers, J., Villa, I., Neff, U., Al-Subbary, A. A., Buettner, A., Hippler, D., and Matter, A.: Holocene ITCZ and Indian monsoon dynamics recorded in stalagmites from Oman and Yemen (Socotra), *Quaternary Sci. Rev.*, 26, 170–188, 2007.

30 Fohlmeister, J., Schröder-Ritzrau, A., Scholz, D., Spötl, C., Riechelmann, D. F. C., Mudelsee, M., Wackerbarth, A., Gerdes, A., Riechelmann, S., Immenhauser, A., Richter, D. K., and Mangini, A.: Bunker Cave stalagmites: an archive for central European Holocene climate variability, *Clim. Past*, 8, 1751–1764, doi:10.5194/cp-8-1751-2012, 2012.

**A 500 year seasonally resolved  $\delta^{18}\text{O}/\delta^{13}\text{C}$** M. Van Rampelbergh  
et al.[Title Page](#)[Abstract](#)[Introduction](#)[Conclusions](#)[References](#)[Tables](#)[Figures](#)[Back](#)[Close](#)[Full Screen / Esc](#)[Printer-friendly Version](#)[Interactive Discussion](#)

Frisia, S., Borsato, A., Preto, N., and McDermott, F.: Late Holocene annual growth in three Alpine stalagmites records the influence of solar activity and the North Atlantic Oscillation on winter climate, *Earth Planet. Sc. Lett.*, 216, 411–424, 2003.

Genty, D. and Quinif, Y.: Annually laminated sequences in the internal structure of some Belgian stalagmites – importance for paleoclimatology, *J. Sediment. Res.*, 66, 275–288, 1996.

Genty, D., Baker, A., and Vokal, B.: Intra- and inter-annual growth rate of modern stalagmites, *Chem. Geol.*, 176, 191–212, 2001.

Genty, D., Blamart, D., Ouahdi, R., Gilmour, M., Baker, A., Jouzel, J., and Van-Exter, S.: Precise dating of Dansgaard–Oeschger climate oscillations in western Europe from stalagmite data, *Nature*, 421, 833–837, 2003.

Jones, P. D. and Mann, M. E.: Climate over past millennia, *Rev. Geophys.*, 42, RG2002, doi:10.1029/2003RG000143, 2004.

Kottek, M., Grieser, J., Beck, C., Rudolf, B., and Rubel, F.: World map of the Koppen–Geiger climate classification updated, *Meteorol. Z.*, 15, 259–263, 2006.

Lassen, K. and Friischristensen, E.: Variability of solar-cycle length during the past 5 centuries and the apparent association with terrestrial climate, *J. Atmos. Terr. Phys.*, 57, 835–845, 1995.

Le Roy Ladurie, E.: *Histoire Humaine et Comparée du Climat, Canucules et Glaciers XIII et XVIII Sciècles*, 2004.

Luterbacher, J., Xoplaki, E., Dietrich, D., Jones, P. D., Davies, T. D., Portis, D., Gonzalez-Rouco, J. F., von Storch, H., Gyalistras, D., Casty, C., and Wanner, H.: Extending North Atlantic Oscillation reconstructions back to 1500, *Atmos. Sci. Lett.*, 2, 114–124, 2001.

Luterbacher, J., Dietrich, D., Xoplaki, E., Grosjean, M., and Wanner, H.: European seasonal and annual temperature variability, trends, and extremes since 1500, *Science*, 303, 1499–1503, 2004.

Mangini, A., Spotl, C., and Verdes, P.: Reconstruction of temperature in the Central Alps during the past 2000 yr from a delta O-18 stalagmite record, *Earth Planet. Sc. Lett.*, 235, 741–751, 2005.

Mann, M. E.: The Earth system: physical and chemical dimensions of global environmental change, in: *Encyclopedia of Global Environmental Change*, edited by: MacCracken, M. C. and Perry, J. S., John Wiley & Sons, Chichester, 514–516, 2002.

**A 500 year seasonally resolved  $\delta^{18}\text{O}/\delta^{13}\text{C}$** M. Van Rampelbergh  
et al.[Title Page](#)[Abstract](#)[Introduction](#)[Conclusions](#)[References](#)[Tables](#)[Figures](#)[Back](#)[Close](#)[Full Screen / Esc](#)[Printer-friendly Version](#)[Interactive Discussion](#)

Mann, M. E., Bradley, R. S., and Hughes, M. K.: Northern Hemisphere temperatures during the past millennium: inferences, uncertainties, and limitations, *Geophys. Res. Lett.*, 26, 759–762, 1999.

Mattey, D., Lowry, D., Duffet, J., Fisher, R., Hodge, E., and Frisia, S.: A 53 year seasonally resolved oxygen and carbon isotope record from a modern Gibraltar speleothem: reconstructed drip water and relationship to local precipitation, *Earth Planet. Sc. Lett.*, 269, 80–95, 2008.

McDermott, F.: Centennial-scale Holocene climate variability revealed by a high-resolution speleothem  $\delta\text{O}-18$  record from SW Ireland (9 Nov, pg 1328, 2001), *Science*, 309, 1816–1816, 2005.

McDermott, F., Atkinson, T. C., Fairchild, I. J., Baldini, L. M., and Mattey, D. P.: A first evaluation of the spatial gradients in  $\delta\text{O}-18$  recorded by European Holocene speleothems, *Global Planet. Change*, 79, 275–287, 2011.

Mook, W. G.: Introduction – theory, methods, review, vol. 1, in: *Environmental Isotopes in the Hydrological Cycle. Principles and Applications*, 2000.

Mühlinghaus, C., Scholz, D., and Mangini, A.: Modelling stalagmite growth and  $\delta\text{C}-13$  as a function of drip interval and temperature, *Geochim. Cosmochim. Ac.*, 71, 2780–2790, 2007.

Mühlinghaus, C., Scholz, D., and Mangini, A.: Modelling fractionation of stable isotopes in stalagmites, *Geochim. Cosmochim. Ac.*, 73, 7275–7289, 2009.

Nicholas, F. J. and Glasspoole, J.: General monthly rainfall over England and Wales, 1727 to 1931, in: *British Rainfall*, 299–306, 1931.

Niggemann, S., Mangini, A., Mudelsee, M., Richter, D. K., and Wurth, G.: Sub-Milankovitch climatic cycles in Holocene stalagmites from Sauerland, Germany, *Earth Planet. Sc. Lett.*, 216, 539–547, 2003.

Perette, Y.: Etude de la Structure Interne des Stalagmites: Contribution a la Connaissance Geographique des Evolutions Environnementales du Vercors (France), *Geographie, Univ. de Savoie, France*, 277 pp., 2000.

Quinif, Y.: Une Nouvelle Topographie de la Grotte de Han, *Lapiaz Hors Serie “Special Han”*, 15–18, 1988.

Rozanski, K., Araguasaraguas, L., and Gonfiantini, R.: Relationship between long-term trends of  $^{18}\text{O}$  isotope composition of precipitation and climate, *Science*, 258, 981–985, 1992.

**A 500 year seasonally resolved  $\delta^{18}\text{O}/\delta^{13}\text{C}$** M. Van Rampelbergh  
et al.[Title Page](#)[Abstract](#)[Introduction](#)[Conclusions](#)[References](#)[Tables](#)[Figures](#)[Back](#)[Close](#)[Full Screen / Esc](#)[Printer-friendly Version](#)[Interactive Discussion](#)

Schmidt, G. A., LeGrande, A. N., and Hoffmann, G.: Water isotope expressions of intrinsic and forced variability in a coupled ocean–atmosphere model, *J. Geophys. Res.-Atmos.*, 112, D10103, doi:10.1029/2006JD007781, 2007.

Scholz, D. and Hoffmann, D. L.: StalAge – an algorithm designed for construction of speleothem age models, *Quat. Geochronol.*, 6, 369–382, 2011.

Scholz, D., Muehlinghaus, C., and Mangini, A.: Modelling delta C-13 and delta O-18 in the solution layer on stalagmite surfaces, *Geochim. Cosmochim. Ac.*, 73, 2592–2602, 2009.

Spotl, C. and Mangini, A.: Stalagmite from the Austrian Alps reveals Dansgaard–Oeschger events during isotope stage 3: Implications for the absolute chronology of Greenland ice cores, *Earth Planet. Sc. Lett.*, 203, 507–518, 2002.

Trouet, V., Esper, J., Graham, N. E., Baker, A., Scourse, J. D., and Frank, D. C.: Persistent positive North Atlantic oscillation mode dominated the medieval climate anomaly, *Science*, 324, 78–80, 2009.

Van Engelen, A. F. V., Buisman, J., and Ijnsen, F.: A millennium of weather, winds and water in the Low Countries, in: *History and Climate, Memories of the Future?*, Kluwer Academics, 2001.

Van Rampelbergh, M., Verheyden, S., Allan, M., Quinif, Y., Keppens, E., and Claeys, P.: Seasonal variations recorded in cave monitoring results and a 10-year monthly resolved speleothem  $\delta^{18}\text{O}$  and  $\delta^{13}\text{C}$  record from the Han-sur-Lesse cave, Belgium, *Clim. Past*, accepted, 2014.

Verheyden, S.: Speleothems as Palaeoclimatic Archives. Isotopic and Geochemical Study of the Cave Environment and its Late Quaternary records, Ph.D. thesis, Vrije Universiteit Brussel, Belgium, 132 pp., 2001.

Verheyden, S., Baele, J.-M., Keppens, E., Genty, D., Cattani, O., Hai, C., Edwards, L., Hucai, Z., Van Strijdonck, M., and Quinif, Y.: The proserpine stalagmite (Han-sur-Lesse cave, Belgium): preliminary environmental interpretation of the last 1000 years as recorded in a layered speleothem, *Geol. Belg.*, 9, 245–256, 2006.

Verheyden, S., Genty, D., Deflandre, G., Quinif, Y., and Keppens, E.: Monitoring climatological, hydrological and geochemical parameters in the Pere Noel cave (Belgium): implication for the interpretation of speleothem isotopic and geochemical time-series, *Int. J. Speleol.*, 37, 221–234, 2008.

Verheyden, S., Keppens, E., Quinif, Y., Cheng, H. J., and Edwards, L. R.: Late-glacial and Holocene climate reconstruction as inferred from a stalagmite – Grotte du Pere Noel, Hans-sur-Lesse, Belgium, *Geol. Belg.*, 17, 83–89, 2014.

Wackerbarth, A., Scholz, D., Fohlmeister, J., and Mangini, A.: Modelling the delta O-18 value of cave drip water and speleothem calcite, *Earth Planet. Sc. Lett.*, 299, 387–397, 2010.

Wagner, S. and Zorita, E.: The influence of volcanic, solar and the Dalton Minimum (1790–1830): CO<sub>2</sub> forcing on the temperatures in a model study, *Clim. Dynam.*, 25, 205–218, 2005.

Wang, Y., Cheng, H., Edwards, R. L., Kong, X., Shao, X., Chen, S., Wu, J., Jiang, X., Wang, X., and An, Z.: Millennial- and orbital-scale changes in the East Asian monsoon over the past 224,000 years, *Nature*, 451, 1090–1093, 2008.

CPD

10, 4149–4190, 2014

## A 500 year seasonally resolved $\delta^{18}\text{O}/\delta^{13}\text{C}$

M. Van Rampelbergh  
et al.

Title Page

Abstract

Introduction

Conclusions

References

Tables

Figures



Back

Close

Full Screen / Esc

Printer-friendly Version

Interactive Discussion



**A 500 year seasonally resolved  $\delta^{18}\text{O}/\delta^{13}\text{C}$**

M. Van Rampelbergh et al.

**Table 1.** U/Th measurements (University of Minnesota) of the Proserpine stalagmite. All ages are converted to before 2013. Ages number 1, 2, 7, 8, 15, 17, 18 and 19, marked in italic are the U/Th-ages from Verheyden et al., 2006.

<sup>230</sup> Th dating results. The error is 2σ error.										
Sample Number	STM PART	Distance mm	<sup>238</sup> U (ppb)	<sup>232</sup> Th (ppt)	<sup>230</sup> Th/ <sup>232</sup> Th (atomic × 10 <sup>-6</sup> )	$\delta^{234}\text{U}^a$ (measured)	<sup>230</sup> Th/ <sup>238</sup> U (activity)	<sup>230</sup> Th Age (yr) (uncorrected)	<sup>230</sup> Th Age (yr) (corrected) <sup>b</sup>	<sup>230</sup> Th Age (yr AD) (corrected)
<i>1</i>	<i>I</i>	<i>15</i>	<i>154.2 ± 0.1</i>		<i>5.2 ± 0.2</i>	<i>1390.7 ± 1.8</i>	<i>0.0036 ± 0.0002</i>	<i>164 ± 8</i>	<i>42 ± 70</i>	<i>1971 ± 70</i>
<i>2</i>	<i>I</i>	<i>60</i>	<i>118.6 ± 0.2</i>		<i>9.8 ± 0.4</i>	<i>1396 ± 4</i>	<i>0.0043 ± 0.0002</i>	<i>194 ± 7</i>	<i>119 ± 44</i>	<i>1894 ± 44</i>
3	I	86	66.8 ± 0.1	1444 ± 29	9 ± 1	1382.8 ± 3.3	0.0118 ± 0.0003	540 ± 13	276 ± 187	1737 ± 187
4	II	112	52.4 ± 0.1	260 ± 5	20 ± 1	1400.4 ± 4.2	0.0060 ± 0.0003	275 ± 13	215 ± 45	1798 ± 45
5	II	130	42.9 ± 0.1	124 ± 3	36 ± 2	1393.0 ± 5.6	0.0063 ± 0.0004	288 ± 17	253 ± 30	1760 ± 30
6	III	195	41.4 ± 0.1	316 ± 6	20 ± 1	1275.9 ± 3.7	0.0091 ± 0.0004	435 ± 17	337 ± 71	1676 ± 71
7	<i>IV</i>	<i>245</i>	<i>42.6 ± 0.1</i>		<i>44 ± 2</i>	<i>1329.4 ± 2.3</i>	<i>0.0087 ± 0.0004</i>	<i>408 ± 17</i>	<i>379 ± 30</i>	<i>1634 ± 30</i>
8	<i>IV</i>	<i>275</i>	<i>57.2 ± 0.1</i>		<i>41 ± 2</i>	<i>1347.7 ± 4.1</i>	<i>0.0092 ± 0.0004</i>	<i>430 ± 18</i>	<i>396 ± 30</i>	<i>1617 ± 30</i>
9	IV	332	65.3 ± 0.1	171 ± 4	55 ± 2	1309.7 ± 4.2	0.0087 ± 0.0003	411 ± 12	378 ± 26	1635 ± 26
10	V	342	55.1 ± 0.1	83 ± 2	94 ± 3	1395.5 ± 3.3	0.0086 ± 0.0002	393 ± 11	374 ± 17	1639 ± 17
11	V	360	38.8 ± 0.1	173 ± 4	38 ± 1	1401.4 ± 4.4	0.0103 ± 0.0003	469 ± 15	415 ± 41	1598 ± 41
12	V	399.2	44.6 ± 0.1	167 ± 3	48 ± 2	1398.5 ± 3.2	0.0108 ± 0.0003	494 ± 15	<b>449 ± 35</b>	<b>1564 ± 35</b>
13	VI	433.5	40.6 ± 0.1	72 ± 2	98 ± 4	1394.2 ± 4.3	0.0106 ± 0.0004	482 ± 18	460 ± 23	1553 ± 23
14	VI	493.5	43.7 ± 0.1	86 ± 2	91 ± 4	1406.2 ± 3.7	0.0109 ± 0.0004	495 ± 17	<b>471 ± 24</b>	<b>1542 ± 24</b>
15	<i>VI</i>	<i>510</i>	<i>46.7 ± 0.1</i>		<i>185 ± 19</i>	<i>1402.9 ± 4.2</i>	<i>0.0096 ± 0.0005</i>	<i>439 ± 23</i>	<i>440 ± 24</i>	<i>1573 ± 24</i>
16	VII	518	38.6 ± 0.1	79 ± 2	88 ± 4	1402.9 ± 4.5	0.0109 ± 0.0005	497 ± 23	<b>472 ± 29</b>	<b>1541 ± 29</b>
17	<i>VII</i>	<i>530</i>	<i>52.3 ± 0.1</i>		<i>184 ± 11</i>	<i>1409.8 ± 3.0</i>	<i>0.0101 ± 0.0004</i>	<i>459 ± 18</i>	<i>460 ± 19</i>	<i>1553 ± 19</i>
18	<i>VII</i>	<i>540</i>	<i>52.6 ± 0.1</i>		<i>188 ± 11</i>	<i>1392.8 ± 3.3</i>	<i>0.0105 ± 0.0004</i>	<i>481 ± 18</i>	<i>482 ± 19</i>	<i>1531 ± 19</i>
19	<i>VII</i>	<i>560</i>	<i>47.5 ± 0.1</i>		<i>219 ± 19</i>	<i>1394.9 ± 4.2</i>	<i>0.0113 ± 0.0005</i>	<i>515 ± 22</i>	<i>517 ± 23</i>	<i>1496 ± 23</i>
20	VII	560	45.9 ± 0.1	42 ± 1	208 ± 10	1384.7 ± 4.1	0.0115 ± 0.0004	525 ± 20	<b>514 ± 21</b>	<b>1499 ± 21</b>

U decay constants:  $\lambda_{238} = 1.55125 \times 10^{-10}$  (Jaffey et al., 1971) and  $\lambda_{234} = 2.82206 \times 10^{-6}$  (Cheng et al., 2013). Th decay constant:  $\lambda_{230} = 9.1705 \times 10^{-6}$  (Cheng et al., 2013).

<sup>a</sup>  $\delta^{234}\text{U} = ((^{234}\text{U}/^{238}\text{U})_{\text{activity}} - 1) \times 1000$ .

<sup>b</sup>  $\delta^{234}\text{U}_{\text{initial}}$  was calculated based on <sup>230</sup>Th age (T), i.e.,  $\delta^{234}\text{U}_{\text{initial}} = \delta^{234}\text{U}_{\text{measured}} \times e^{\lambda_{234} \times T}$ .

Corrected <sup>230</sup>Th ages assume the initial <sup>230</sup>Th/<sup>232</sup>Th atomic ratio of  $4.4 \pm 2.2 \times 10^{-6}$ . Those are the values for a material at secular equilibrium, with the bulk earth <sup>232</sup>Th/<sup>238</sup>U value of 3.8. The errors are arbitrarily assumed to be 50 %.

<sup>b</sup> Ages are reported before 2013.

Title Page

Abstract

Introduction

Conclusions

References

Tables

Figures

⏪

⏩

⏴

⏵

Back

Close

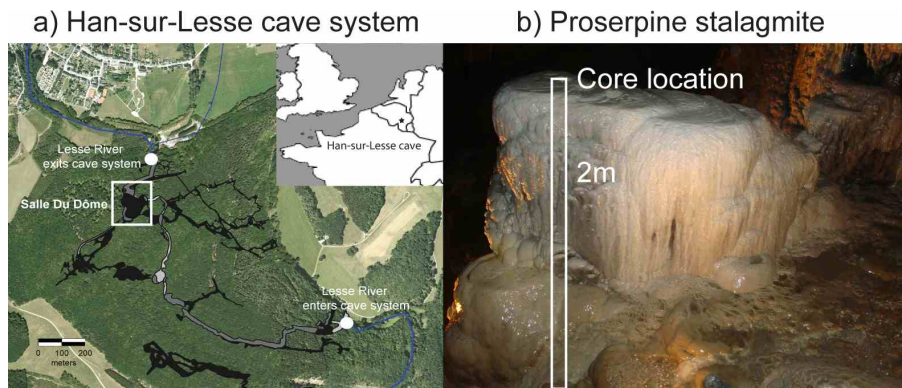
Full Screen / Esc

Printer-friendly Version

Interactive Discussion

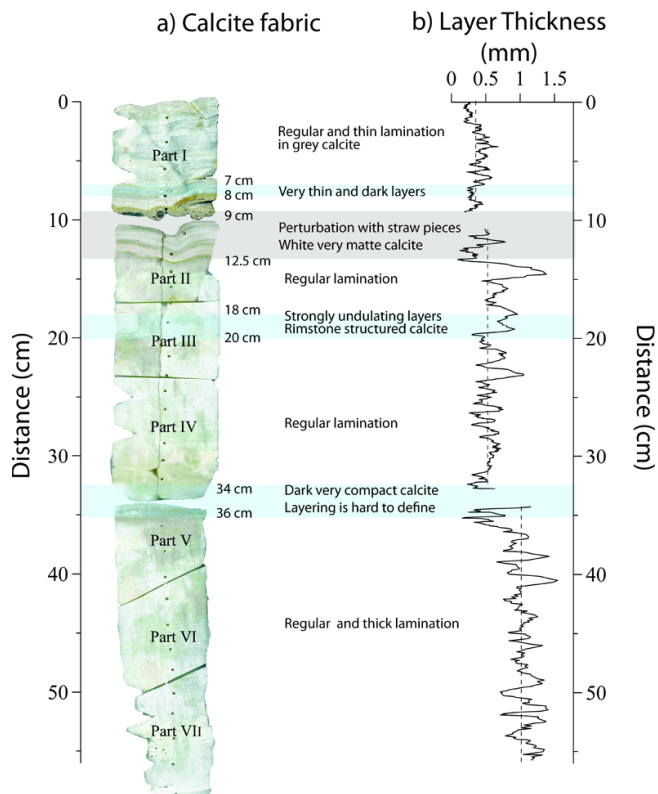




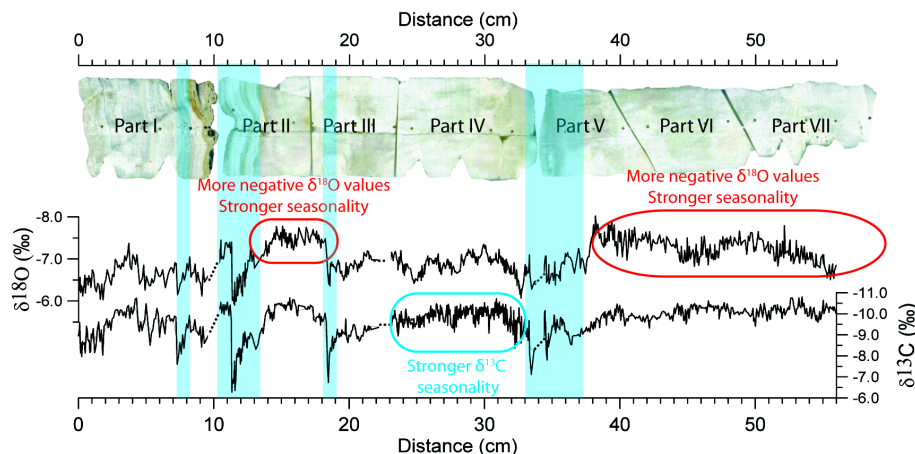
**A 500 year seasonally resolved  $\delta^{18}\text{O}/\delta^{13}\text{C}$** M. Van Rampelbergh  
et al.

**Figure 1.** (a) The Han-sur-Lesse cave system is located in the southern part of Belgium. The Proserpine stalagmite was sampled in the Salle-du-Dôme chamber (white square) located 500 m from the cave exit. (b) The Proserpine stalagmite with the location of the 2 m long core that was drilled in 2001 at the spot where most of the drip water falls.

[Title Page](#)[Abstract](#)[Introduction](#)[Conclusions](#)[References](#)[Tables](#)[Figures](#)[◀](#)[▶](#)[◀](#)[▶](#)[Back](#)[Close](#)[Full Screen / Esc](#)[Printer-friendly Version](#)[Interactive Discussion](#)



**Figure 2.** (a) Calcite fabric and layer thickness of the Proserpine stalagmite for the different parts (I to VII). Between 9 and 12.5 cm, calcite deposition is strongly disturbed and straw pieces are embedded in the calcite. Part I, located above the perturbation, displays darker and more compact calcite compared to the parts II to VII, below the perturbation. Strongly undulating layers occur between 18 and 20 cm. (b) Layer thickness averages  $0.3 \text{ mm layer}^{-1}$  in part I,  $0.5 \text{ mm layer}^{-1}$  in the parts II to IV and  $1 \text{ mm layer}^{-1}$  in the parts V to VII. Thin layers of  $0.2 \text{ mm layer}^{-1}$  occur from 7 to 8 cm and from 34 to 36 cm.

A 500 year seasonally resolved  $\delta^{18}\text{O}/\delta^{13}\text{C}$ M. Van Rampelbergh  
et al.

**Figure 3.** The Proserpine  $\delta^{18}\text{O}$  and  $\delta^{13}\text{C}$  composition reported in ‰ VPDB plotted against distance from top. The two measured proxies display a good correlation in part I. In the parts II to VII, the  $\delta^{18}\text{O}$  and  $\delta^{13}\text{C}$  values evolve more differently. The  $\delta^{18}\text{O}$  values display two periods of more negative values with stronger seasonality between 14 and 18.5 cm and between 38 and 56 cm. The  $\delta^{13}\text{C}$  values vary around  $-10 \pm 0.12$ ‰ and display stronger seasonality between 32 and 27 cm. Four periods where both the  $\delta^{18}\text{O}$  and the  $\delta^{13}\text{C}$  values display an abrupt increase to  $-6.0 \pm 0.16$  and  $-8.0 \pm 0.12$ ‰ respectively, are indicated by the blue bars.

Title Page

Abstract

Introduction

Conclusions

References

Tables

Figures



Back

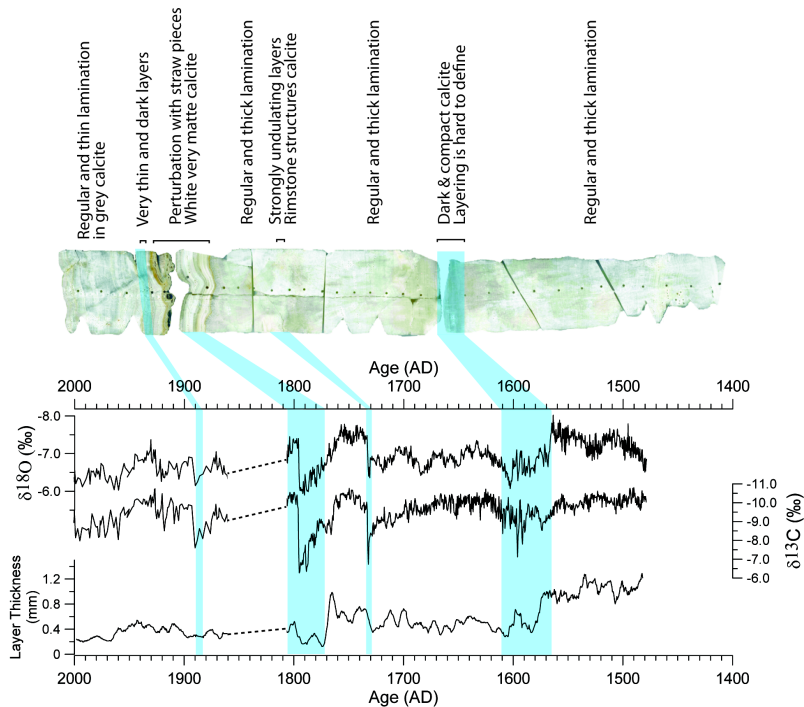
Close

Full Screen / Esc

Printer-friendly Version

Interactive Discussion

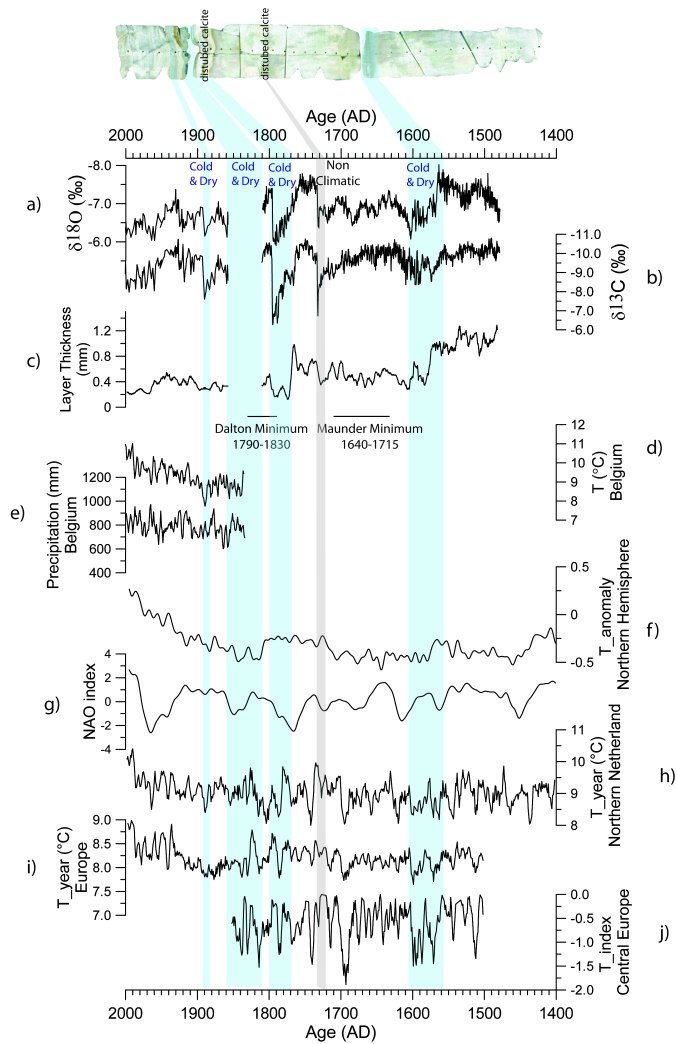




**Figure 4.** Comparison between the  $\delta^{18}\text{O}$  and  $\delta^{13}\text{C}$  values in ‰ VPDB, layer thickness and calcite fabric of the Proserpine. During the anomalies between 1565 and 1610, at 1730, between 1770 and 1800 and between 1880 and 1895 (blue bars), the  $\delta^{18}\text{O}$  and  $\delta^{13}\text{C}$  values increase, layers become thinner and calcite fabric is darker or heavily disturbed. With the exception of the anomalies the  $\delta^{18}\text{O}$ ,  $\delta^{13}\text{C}$  and layer thickness values display lower amplitude variations. Sampling for the  $\delta^{18}\text{O}$  and  $\delta^{13}\text{C}$  values was done layer per layer between 1810 and 1479 and signals reflect seasonal variations.

## A 500 year seasonally resolved $\delta^{18}\text{O}/\delta^{13}\text{C}$

M. Van Rampelbergh  
et al.


[Title Page](#)
[Abstract](#)
[Introduction](#)
[Conclusions](#)
[References](#)
[Tables](#)
[Figures](#)

[Back](#)
[Close](#)
[Full Screen / Esc](#)
[Printer-friendly Version](#)
[Interactive Discussion](#)


---

**A 500 year seasonally resolved  $\delta^{18}\text{O}/\delta^{13}\text{C}$** 

M. Van Rampelbergh  
et al.

---

**Figure 5.** The **(a)**  $\delta^{18}\text{O}$  and **(b)**  $\delta^{13}\text{C}$  composition reported in ‰ VPDB and **(c)** layer thickness plotted against **(d)** the instrumental temperature and **(e)** precipitation record of the Belgian Royal Meteorological Institute (RMI) measured since 1833 **(f)** the Northern Hemisphere temperature reconstruction (Jones and Mann, 2004), **(g)** the winter NAO index reconstruction (Trouet et al., 2009), **(h)** a temperature reconstruction from the northern Netherlands based on different instrumental and historical archives (Van Engelen et al., 2001), **(i)** the yearly temperature reconstruction in Europe (Luterbacher et al., 2004) and **(j)** the temperature reconstruction of central Europe (Dobrovolny et al., 2010). Three anomaly periods with less negative  $\delta^{18}\text{O}$  and  $\delta^{13}\text{C}$  values and thinner layers occur between 1565 and 1610, 1770 and 1800 and between 1880 and 1895 (indicated in blue) and are interpreted to reflect colder and drier winter periods. The perturbation between 1810 and 1860 is also interpreted as an anomaly and reflects exceptionally cold and dry winter conditions (also indicated in blue). The anomaly at 1730 does not correspond with climate variations and is suggested driven by non-climatic factors (grey bar). Two periods of warmer and wetter winters occur from 1479 and 1565 and from 1730 to 1770 separated by a period with cooler and drier winters between 1610 and 1730. A decrease in  $\delta^{18}\text{O}$  seasonality in the colder and drier period between 1610 and 1730 indicates lower cave air temperature seasonality than during the warmer and wetter winter periods (1479–1565 and 1730–1770). Seasonality in the  $\delta^{13}\text{C}$  signal is higher between 1600 and 1660 and indicates more intense PCP during summer, which is caused by decreased winter recharge.

[Title Page](#)[Abstract](#)[Introduction](#)[Conclusions](#)[References](#)[Tables](#)[Figures](#)[Back](#)[Close](#)[Full Screen / Esc](#)[Printer-friendly Version](#)[Interactive Discussion](#)